Publishing House
AKAPIT

COMPUTER METHODS IN MATERIALS SCIENCE

Informatyka w Technologii Materiałów

Vol. 10, 2010, No. 1

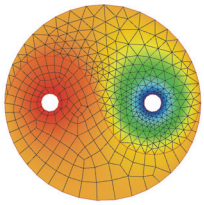

STABILITY AND UNIQUENESS OF FLOW APPROACH ALGORITHMS IN SHEET METAL FORMING SIMULATIONS

WŁODZIMIERZ SOSNOWSKI[1,2], TOMASZ BEDNAREK[1,2*], PIOTR KOWALCZYK[1]

[1] Institute of Fundamental Technological Research PAN, Warsaw, ul. Pawińskiego 5b
[2] Kazimierz Wielki University, Bydgoszcz, ul. Chodkiewicza 30
**Corresponding Author: bednarek@ippt.gov.pl*

Abstract

The objective of this paper is to improve stability conditions, uniqueness and convergence of the flow approach algorithm with rigid-viscoplastic and plastic material models. Two numerical codes, MFP2D and MFP3D, were used previously for practical industrial solutions (Sosnowski, 2001; Sosnowski, 1995; Sosnowski et al., 1992). Relative simplicity of both the codes allowed to include "exact" sensitivity calculations by direct differentiation method. This made it possible to perform very effective optimization of the whole sheet metal forming process simulation. One of significant drawbacks of rigid-viscoplastic shell approach is poor stability and convergence due to relatively high values of the condition number of the resulting system of equations. The reasons include the absence of elasticity terms in the constitutive material law and asymptotic character of the relationship between viscosity and effective plastic strain rate. Approximate character of the contact modeling (penalty approach) also affects conditioning of the system. This drawback can be overcome by some measures proposed in this paper.

Key words: sheet drawing, flow approach, matrix condition number

1. INTRODUCTION

The objective of this paper is the improvement of the flow approach algorithm employed in sheet metal forming simulation software MFP2D and MFP3D. The stable solution using MFP2D/3D could be obtained upon deep study of algorithm properties and two constitutive laws employed there: rigid-viscoplastic and rigid-plastic.

In previous investigations the influence of the rigid part movement of the drawing sheet to the conditioning of the solution was examined. Special attention was paid to asymptotic character of both the constitutive laws. The singularities lead to unstable solution for both very small and large viscosities (Sosnowski, 1995).

In this study, procedures for evaluation of norms of the right hand side vectors were elaborated. Conditioning of the solution was examined for different norms. A few vector-based norms of the stiffness matrix were also investigated. Variation of the norms and matrix condition number defined on the basis of these norms were estimated for a simple benchmark drawing tests.

The final effect of the investigations should be the improvement of the nonlinear solutions using MFP2D/3D, their precision and uniqueness.

2. GENERAL SYSTEM OF EQUATIONS IN THE FLOW APPROACH ALGORITHM

The discretized viscoplastic shell finite element equations for velocities $\dot{\mathbf{u}}$, nodal velocities $\dot{\mathbf{a}}$, strain rates $\dot{\boldsymbol{\varepsilon}}$ and stresses $\boldsymbol{\sigma}$, are written as

ISSN 1641-8581

$$\dot{\mathbf{u}} = \varphi\dot{\mathbf{a}}$$
$$\dot{\boldsymbol{\varepsilon}} = \mathbf{B}\dot{\mathbf{a}} \qquad (1)$$
$$\boldsymbol{\sigma} = \mathbf{E}(\overline{G},\overline{\nu})\dot{\boldsymbol{\varepsilon}} = \mathbf{E}(\overline{G},\overline{\nu})\mathbf{B}\dot{\mathbf{a}}$$

In equations (1) $\boldsymbol{\varphi}$ is the shape function matrix, $\mathbf{B}$ is the standard "strain" matrix of infinitesimal shell or membrane theory which defines dependence between strain rate vector and nodal velocities. The elements of $\mathbf{B}$ matrix are shape function derivatives with respect to coordinates x, y and z in constant, orthogonal coordinate system. $\mathbf{E}(\overline{G},\overline{\nu})$ is the constitutive matrix of viscoplastic material. The form of $\mathbf{E}(\overline{G},\overline{\nu})$ depends on the assumed model of viscous shell (membrane or bending). In the more simple, membrane case (employed in this paper) we have (Sosnowski, 1995)

$$\mathbf{E}(\overline{G},\overline{\nu}) = \frac{2\overline{G}h}{1-\overline{\nu}}\begin{bmatrix} 1 & \overline{\nu} & 0 \\ \overline{\nu} & 1 & 0 \\ 0 & 0 & \dfrac{1-\overline{\nu}}{2} \end{bmatrix} \qquad (2)$$

$\overline{G}$ and $\overline{\nu}$ are the equivalent material parameters precisely corresponding to the elastic shear modulus and the Poisson's ratio in analogous elastic shell (Onate & Agelet de Saracibar, 1990; Onate & Zienkiewicz, 1983; Onate et al., 1988).

The general FEA system of equations is obtained in standard form

$$\mathbf{K}\dot{\mathbf{a}} = \mathbf{Q} \qquad (3)$$

with $\mathbf{K}$ and $\mathbf{Q}$ denoting the secant stiffness matrix and the external nodal force vector of the viscoplastic shell, respectively.

In fact, equation (3) is a nonlinear system of equations due to the nature of material parameters $\overline{G}$ and $\overline{\nu}$, of which at least $\overline{G}$ is a function of $\dot{\boldsymbol{\varepsilon}}$, cf. (6), which results in $\mathbf{K} = \mathbf{K}(\dot{\mathbf{a}})$. The solution of (3) can be attempted via direct or incremental iterative solution techniques. The exact form of the tangent matrix for the general nonlinear voided case is extremely complex and therefore secant and pseudo-secant methods are more appropriate (Sosnowski, 1995). The simplest solution technique is based on a direct scheme giving for the i-th iteration (Sosnowski, 2001)

$$\Delta\dot{\mathbf{a}}^{i+1} = -[\mathbf{K}^i]^{-1}\mathbf{R}^i \qquad (4a)$$
$$\dot{\mathbf{a}}^{i+1} = \dot{\mathbf{a}}^i + \Delta\dot{\mathbf{a}}^{i+1} \qquad (4b)$$

check convergence

In the above scheme $\mathbf{R}^i$ is the standard residual force vector computed as

$$\mathbf{R}^i = \int_\Omega \mathbf{B}^T\boldsymbol{\sigma}^i d\Omega - \mathbf{Q}^i \qquad (5)$$

Once the converged velocity field has been found from equation (4b), the sheet geometry and boundary conditions are updated and the process is restarted. This process allows to treat contact and friction conditions in a simple manner.

3. CONVERGENCE PROBLEMS IS FLOW APPROACH ALGORITHM

The convergence of the system of nonlinear equations solution is usually controlled by residual forces criterion. Sosnowski (1995) proposed the new criterion based on the velocity norm. The advantage of velocity norm criterion is clearly shown in a simple axisymmetric deep drawing example (figure 1) where the graph of the velocity norm versus the residual force vector norm for a typical solution step is shown. We can see that after about 13 iteration steps (the numbers near dots correspond to iteration number in figure 1), velocity norm is almost constant (a value within range <1.305;1.31>). Simultaneously, the range of consecutive residual norms is relatively wide. Note that the residual norm axis is logarithmically scaled. Both norms, velocities and residual forces, are understood as the well known Euclidean norm.

The converged solution of the system of nonlinear equations is approached faster when using velocity norm criterion than with the residual forces norm criterion. Relatively large oscillations of residual forces are caused by the fact that the same nodes in consecutive iterations switch from the state of contact with tools to the separation state and vice-versa in a staggered manner. Thus, residual forces are not stable.

The effect of unstable residual forces in converged solution can be also explained with the asymptotic form of the expression for the viscosity (equivalent shear modulus)

$$\overline{G} = \frac{\sigma_0}{3\dot{\bar{\varepsilon}}} \qquad (6)$$

where σ_0 is the yield limit and $\dot{\bar{\varepsilon}}$ is a scalar measure of the strain rate tensor. In case of deformation of nearly rigid body, $\dot{\bar{\varepsilon}} \approx 0$, the value of $\overline{G}$ grows asymptotically to infinity. In order to avoid singularity which corresponds to deformation of rigid body,

the cut off value $\overline{G}^*$ of $\overline{G}$ function must be used. This value can be established by numerical experiments for instance as a function of rigid zone area (greater rigid zone area corresponds to smaller equivalent strain rate and thus higher value of $\overline{G}^*$).

In some cases, when strain rates are zero or relatively small, the viscosity function $\overline{G}$ is generally very sensitive even to slight changes in the velocity field. Due to this fact, residual forces are unstable and convergence is poor.

In order to establish optimum convergence tolerance, Sosnowski (1995) made a series of numerical tests.

First, the axisymmetric deep drawing benchmark test proposed by Waggoner (Hora & Krapoth, 1991) has been calculated with the three different convergence tolerance norms:

– convergence tolerance of velocity error norm, $tolerv = 0.01$ (VN01),
– convergence tolerance of velocity error norm, $tolerv = 0.001$ (VN001),
– convergence tolerance of residual force error norm, $tolerf = 0.01$ (ERN01).

The value of tolerances are

$$tolerv = \frac{dvel}{vel}, \qquad tolerf = \frac{resid}{fwew} \tag{7}$$

dvel, *vel*, are respectively norm of velocity increment vector, velocity vector, *resid* and *fwew* are residual forces and internal forces vector. All norms were calculated as typical Euclidean norm.

The convergence condition is assumed on the basis of the relative error. The termination conditions of the iterative process are

$$\frac{dvel_i}{vel_i} \le tolerv \quad \text{or} \quad \frac{resid_i}{fwew_i} \le tolerf \tag{8}$$

where *i* denotes iteration step number.

The new convergence conditions were examined empirically – by calculating the same examples using different convergence criterions. Results of the numerical tests are presented in figures 2 and 3.

The sheet has been modeled with axisymmetric membrane elements. Figure 2 shows some typical results of thickness and equivalent plastic strain for deformed configuration obtained with three mentioned tolerances.

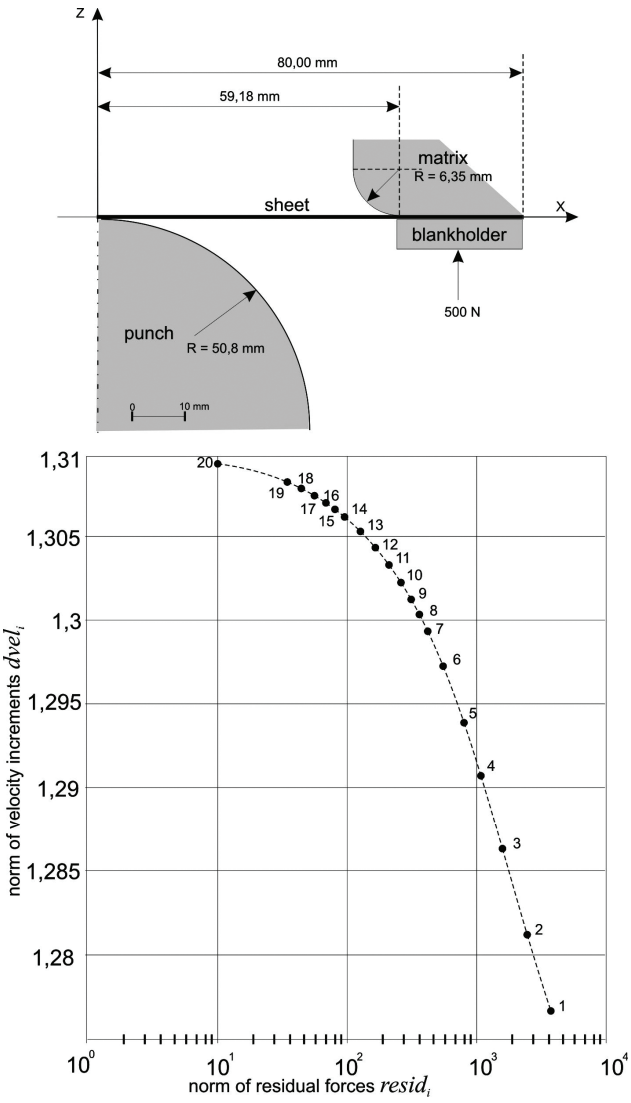

Fig. 1. *Norms of velocities increments and residual forces.*

Distance on horizontal axis on figures 2.3 and 2.4 is calculated along the symmetry line of specimen (see figure 1). All points of discretization for this example are taken into account and equivalent plastic strain is associated with these concrete points of the sheet. Figures 2.1 and 2.2 just show deformed shape of the sheet metal which is presented for punch travel 30 mm and time of step 60s. Draw-in values (2.4 mm for velocity norm VN001, $tolerv = 0.001$ and 2.39 mm for ERN01, $tolerf = 0.01$) are also shown for these two cases.

If we consider two different tolerances: $tolerv = 0.001$ and $tolerf = 0.01$ we can observe that the thickness and equivalent plastic strain distributions differ only very slightly. The number of iterations for the case of the tolerance based on velocity norm $tolerv = 0.001$ is, however, much smaller.

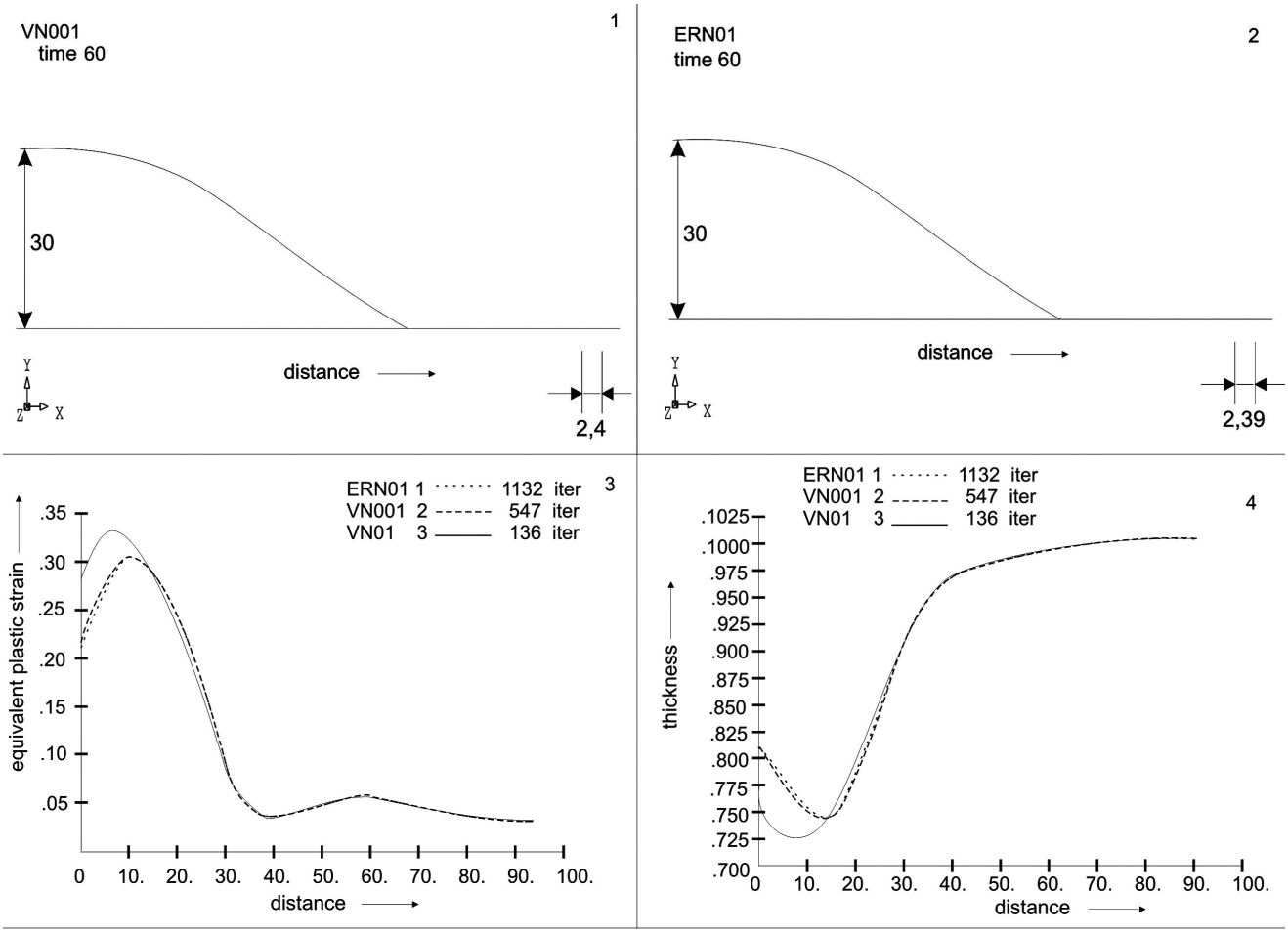

Fig. 2. *Axisymmetrical deep drawing test results for different convergence tolerance norms (Sosnowski, 1995).*

Similar membrane calculations were made with 3D example: cylindrical deep drawing presented in figure 3. Again the differences of thickness, equivalent plastic strain distributions and draw-in values for $tolerv = 0.001$ and $tolerf = 0.01$ are almost invisible. Figures 3.1 and 3.2 show the final drawpiece obtained using respectively: residual forces norm ERN01 and velocity norm VN001. The result of drawing is almost the same for residual forces and velocity norm. Figures 3.3 and 3.4 shows the same values as described above figures 2.3 and 2.4.

The number of iterations which can be saved if the velocity tolerance norm is used instead that of force tolerance norm is much bigger in 3D cases. For typical membrane computations the number of iterations needed when the velocity norm is used is about 19% of that needed for the residual norm case.

4. MATRIX CONDITION NUMBER

The stability and convergence of the iterative algorithm (4) which allows to find increments $\dot{\mathbf{a}}$ are significantly influenced by the solution error of each system of linear equations (4a). This error depends, among other factors, on the condition number of the system coefficients matrix, the equivalent stiffness matrix $\mathbf{K}^i$ (Kincaid & Cheney, 2006). The matrix condition number is given by formula (index i is neglected)

$$\kappa(\mathbf{K}) = \|\mathbf{K}\| \cdot \|\mathbf{K}^{-1}\| \tag{9}$$

where operator $\|\cdot\|$ denotes one of the standard matrix norms, for example

$$\|\mathbf{K}\|_1 = \max_{1\le i,j\le n} |K_{ij}| \quad \text{or} \quad \|\mathbf{K}\|_\infty = \max_{1\le i\le n} \sum_{j=1}^{n} |K_{ij}| \tag{10}$$

The high values of matrix condition number induce higher errors of numerical calculations. The mathematical model should be formulated in a way ensuring the matrix condition number κ to be as small as possible.

The above defined coefficient matrix condition number $\kappa(\mathbf{K}^1)$ was tracked in consecutive iteration steps. The numerical example is a simple two-dimensional sheet model presented in figure 4. The model was discretized with three finite elements.

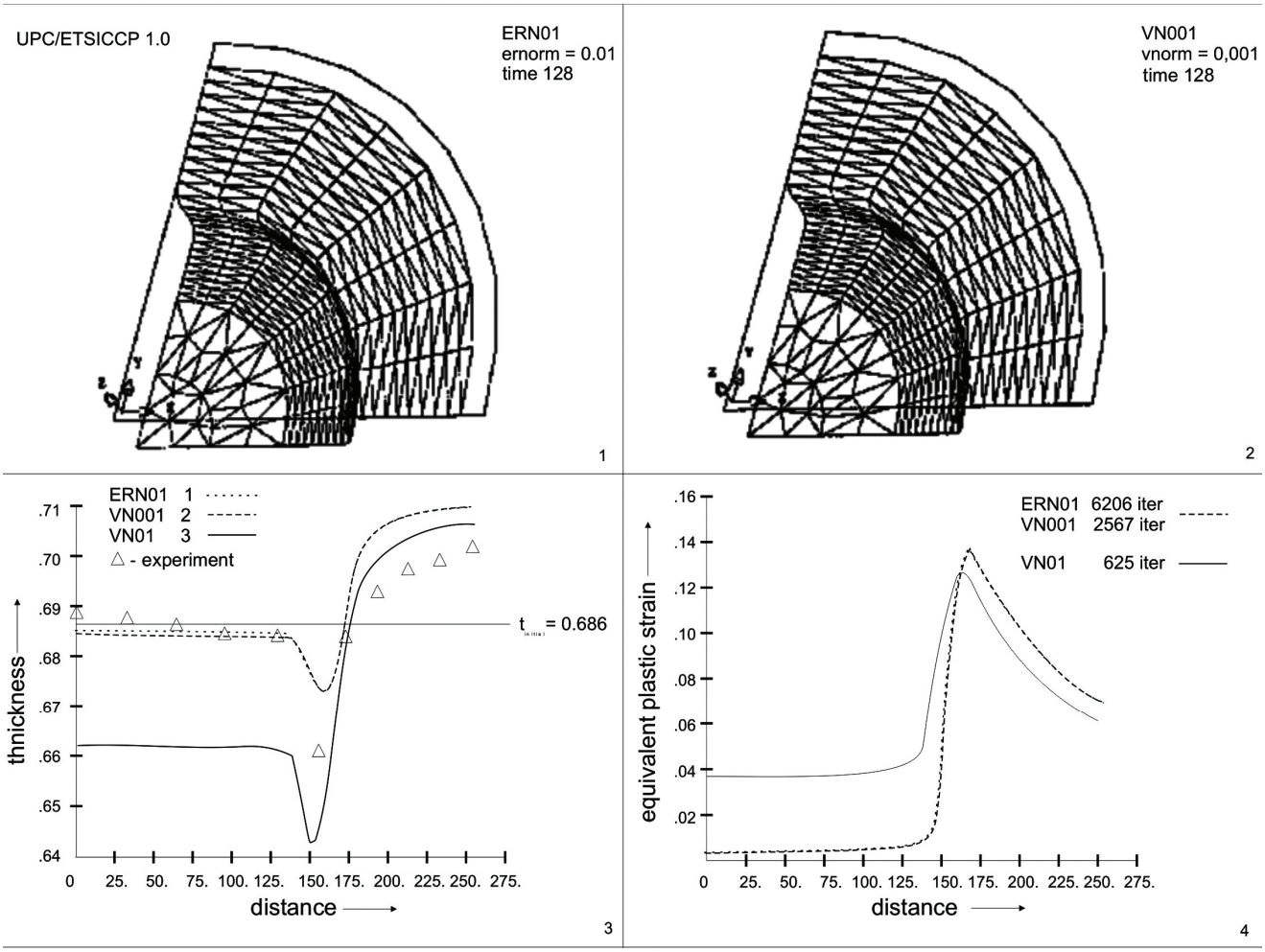

Fig. 3. *Simulation of sheet drawing, 3D specimen (Sosnowski, 1995).*

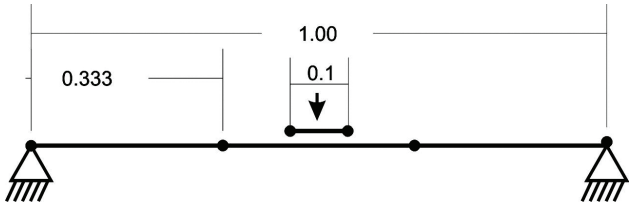

Fig. 4. *Numerical example, 2D sheet drawing.*

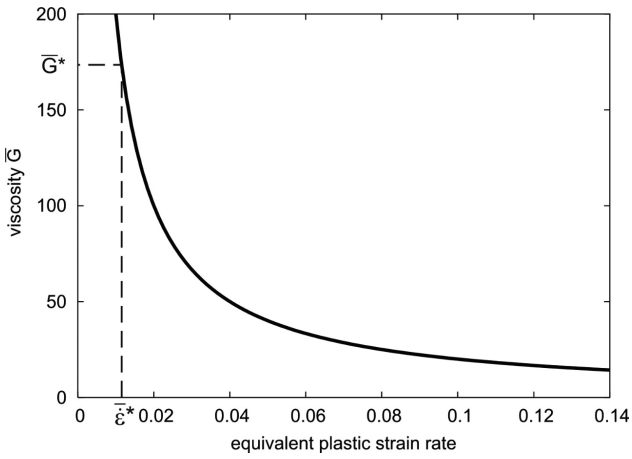

Fig. 5. *Dependency between plastic strain rate and material viscosity.*

There are three (two translational and one rotational) degrees of freedom in each node. The rigid-viscoplastic material model without hardening has been assumed. The viscosity $\overline{G}$ is calculated using formula (6). The value of $\overline{\nu}$ was assumed as $\overline{\nu} = 0.5$. The dependence of $\overline{G}$ on strain ratio is presented in figure 5.

The penalty method was used in order to define contact model. This method does not increase the number of degrees of freedom of the system. Thus, in spite of number of contact conditions the size of the problem was the same. The main system of equations (3) was modified into the form

$$(K_{ij} + \phi\delta_{ki}{}^{T}\delta_{ki})a_j = Q_i + \phi\delta_{ki}\hat{a}_k \qquad (11)$$

where ϕ is penalty factor and $\hat{a}_k$ is assumed condition on k-th degree of freedom.

The choice of the proper value of the penalty factor ϕ is one of the main problems in calculations using contact model based on penalty method. A too small value of ϕ causes bad accuracy of contact modeling. In extreme cases contact might not occur

at all in the model. Assumption of a too large value of ϕ leads to poor system conditioning and significant errors.

The influence of the penalty factor ϕ on the equivalent stiffness matrix condition was examined. The chart of the matrix condition number using different ϕ values in the consecutive iteration steps is presented in figure 6.

ACKNOWLEDGMENTS

This work was partially financed by European Regional Development Fund within the framework Innovative Economy Programme, project number POIG.01.03.01-14-209/09.

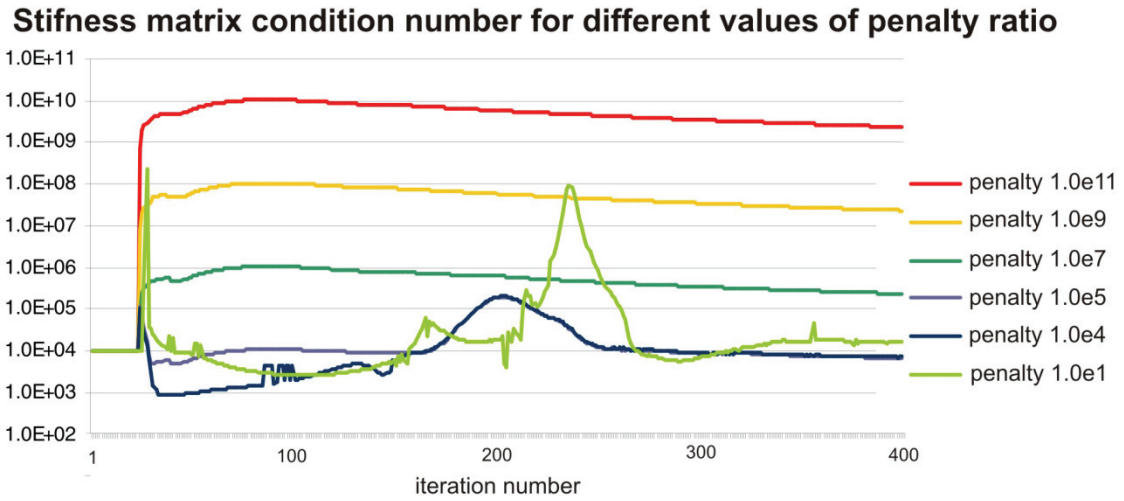

Fig. 6. *Influence of the penalty ratio value on stiffness matrix condition.*

We can see (figure 6) that increasing of penalty factor considerably worsens the condition of the system of equations. The optimum value of penalty $\phi \approx 10^4$ doesn't cause significant deterioration of the system condition while the contact geometry is still correctly represented. A too small value of the penalty factor causes instability of the solution and, in consequence, significant errors in numerical results.

5. CONCLUSIONS

1) One of important drawbacks of the flow approach is poor stability and convergence of FEA solutions.
2) There are many reasons for this. Rigid body motions inside the deformed blank, absence of elastic terms in the constitutive equations, and approximate contact modeling are mostly blamed for these problems.
3) Drawbacks mentioned above can be overcome by minimization of the condition number, e.g. by optimization of the penalty parameter in the contact algorithm.
4) In the paper, simple trial and error procedures of this optimization are proposed.

REFERENCES

Hora P., Krapoth A.,1991, *FE-Simulation of 3D Sheet Metal Forming processes in the Automative Industry*, VDI Benchmark, Institut fur Umformtechnik ETH-2, Zurich.

Kincaid D., Cheney W., 2006, *Analiza numeryczna*, WNT, Warszawa (in Polish).

Onate E., Agelet de Saracibar C., 1990, Analysis of sheet metal forming problems using a selective bending-membrane formulations, *Int. J. Num. Meth. Eng.*, 30, 1577-1593.

Onate E., Kleiber M., Agelet de Saracibar C.,1988, Plastic and viscoplastic flow of void containing metals: Applications to axisymmetric sheet forming problems, *Int. J. Num. Meth. Engng.*, 25, 225-251.

Onate E., Zienkiewicz O.C.,1983, A viscous shell formulation for the analysis of thin sheet metal forming, *Int. J. Mech. Sci.*, 25, 305-335

Sosnowski W., 2001, *Symulacja numeryczna, analiza wrażliwości i optymalizacji nieliniowych procesów deformacji konstrukcji*, Wydawnictwo AB, Bydgoszcz (in Polish).

Sosnowski W.,1995, Finite element simulation of industrial sheet metal forming processes, *Prace IPPT*, 17, IPPT, Warszawa.

Sosnowski W., Onate E., Agelet de Saracibar C., 1992, Comparative study on sheet metal forming processes by numerical modeling and experiment, *J. Materials Processing Technology*, 34, 109-116.

BADANIE STABILNOŚCI I JEDNOZNACZNOŚCI ALGORYTMÓW TEORII PLASTYCZNEGO PŁYNIĘCIA STOSOWANYCH W SYMULACJI TŁOCZENIA BLACH

Streszczenie

W niniejszej pracy rozważamy problem zbieżności i jednoznaczności rozwiązania nieliniowego problemu symulacji procesów tłoczenia blach modelowanych z wykorzystaniem sztywno-lepkoplastycznego modelu materiału. Do symulacji wykorzystujemy programy MFP2D i MFP3D sprawdzone w kilku zastosowaniach przemysłowych (Sosnowski, 2001; Sosnowski, 1995; Sosnowski et al., 1992). Zaletą obydwu kodów numerycznych jest względna prostota algorytmu, a co za tym idzie możliwość dokładnej analizy wrażliwości i optymalizacji procesu tłoczenia blach. Niestety oba programy mają poważną wadę związaną z przyjętym modelem materiału. W trakcie obliczeń obserwujemy niestabilność wywołaną stosunkowo wysokim wskaźnikiem uwarunkowania macierzy układu równań. Dodatkowo przyjęty model kontaktu zawierający funkcję kary pogarsza wskaźnik uwarunkowania macierzy sztywności. Celem badań jest między innymi poprawienie tego wskaźnika.

Received: February 15, 2010
Received in a revised form: April 19, 2010
Accepted: April 22, 2010